

MULTIGAMMA-RAY EVENTS AT THE CERN ISR

G.F. DELL¹ and L.C.L. YUAN¹

Brookhaven National Laboratory, Upton, NY, USA

L.E. ROBERTS² and J. DOOHER²

Adelphi University, Garden City, NY, USA

E. AMALDI, M. BENEVENTANO, B. BORGIA, A. CAPONE, F. DE NOTARISTEFANI,
U. DORE, F. FERRONI, E. LONGO, L. LUMINARI, P. PISTILLI and I. SESTILI

*Istituto di Fisica "G. Marconi" dell'Università, and Istituto Nazionale di Fisica Nucleare,
Sezione di Roma, Roma, Italy*

Received 30 March 1982
(Revised 28 June 1982)

Results of a search for multigamma-ray events at $\sqrt{s} = 52$ GeV in pp collision are reported. The results are compared with a Monte Carlo simulation of the decay of pairs of heavy mass particles by gamma-ray emission, and upper limits for the production cross section are determined.

1. Introduction

In this paper we report the result of a search for high multiplicity gamma-ray events in pp collision at the ISR for $\sqrt{s} = 52$ GeV. In particular we compare the observed photon multiplicity distribution with that expected from the annihilation into a photon shower of magnetic pole-antipole pairs.

From the analysis of the experimental data we obtain upper limits on the production of pole-antipole pairs in the pair mass interval 15–40 GeV for different values of the magnetic pole strength.

In sect. 2 we give a description of the experimental set up, in sect. 3 the analysis of the data. Sect. 4 contains the discussion of the results (table 2).

¹ Research supported by the US NASA and US Department of Energy (former ERDA).

² Work supported in part by US Energy Research and Development Administration contract no. E(11-1) 4604.

2. Experimental set up

The detector consists of seven hodoscopes of lead glass Čerenkov counters, scintillation counters, and multiwire proportional chambers (figs. 1 and 2) and is a rearrangement of the detector described in previous papers [1]. Four hodoscopes, SP, S, F1 and F2 are located at 90° with respect to the circulating beams, while the remaining hodoscopes, U1, U2 and U3 are located at small angles with respect to the beams.

The SP unit was located on the outside of the interaction region. It consisted of nine planes of wire chambers, a 1 cm thick layer of scintillation counters, and a 6×11 array of lead glass blocks each having dimensions of $(10.3 \text{ cm})^2 \times 35 \text{ cm}$ long.

The S unit was located on the inside of the intersection region, while the F1 and F2 units were located above and below the intersection region, respectively. The S, F1 and F2 units each contained a 2×10 array of lead glass blocks. The blocks in the S unit were $(10.3 \text{ cm})^2 \times 35 \text{ cm}$ long, and the blocks in the F1 and F2 units were $(10.3 \text{ cm})^2 \times 50 \text{ cm}$ long. All units had a 1 cm thick layer of scintillation counters in front of the lead glass array. In addition, the S unit contained seven planes of wire chambers, and the F1 and F2 units each contained five planes of wire chambers.

The U1 and U2 units were positioned on the same side of the intersection region with the U1 unit being above the beam plane and the U2 unit being below the beam plane. Each of these units contained 16 blocks of lead glass each measuring $7.5 \text{ cm} \times 15.0 \text{ cm} \times 35 \text{ cm}$ long. The blocks were arranged in four rows each containing four blocks. The blocks in each row were closely spaced; the rows were separated by 5 cm and were oriented so that the midplane of each row passed through the interaction region. A scintillation counter was positioned in front of each lead glass block.

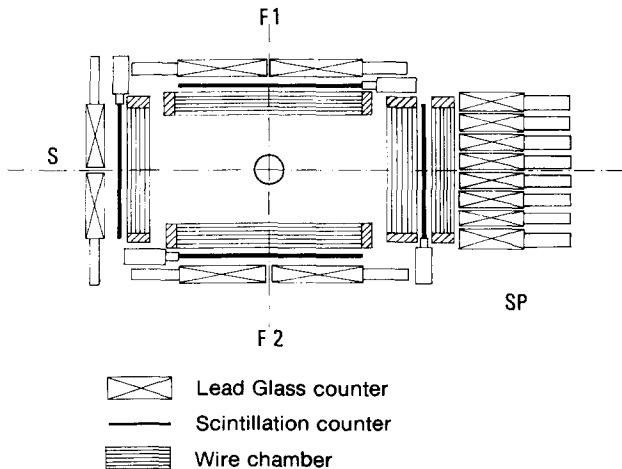


Fig. 1. Vertical section of the apparatus showing the position of various detectors in the middle plane of the interaction region.

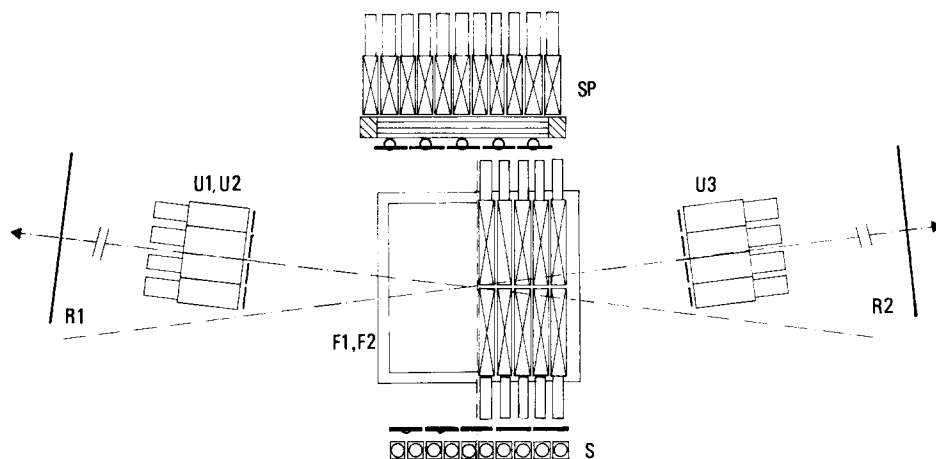


Fig. 2. Top view of the apparatus. Only one half of the Čerenkov counters of F1, F2 is drawn.

The U3 unit consisted of a 4×5 array of $(10.3 \text{ cm})^2 \times 35 \text{ cm}$ long lead glass blocks with a 1 cm thick layer of scintillation counters in front of the lead glass. This unit was positioned on the opposite side of the intersection region from the U1 and U2 units, and it was located below the beam plane.

Finally, two 1 m^2 scintillation counters, R1 and R2, were located 4.5 m downstream of the interaction region in beam one and beam two, respectively. The beam pipes passed through the center of these counters. These counters were connected to time to digital converters and the relative timing was used to identify events originating in the interaction region.

All seven hodoscope units were mounted on chariots that were moved by remote control. To minimize darkening of the lead glass due to radiation, all chariots were retracted from the interaction region during beam injection, beam tuning, and beam dumping.

The lead glass counters were calibrated in electron beams before and after the experiment [2]. Blocks of the SP, U1, U2 and U3 units were calibrated with electrons incident along the longitudinal axis of the blocks; blocks of the S, F1 and F2 units were calibrated with electrons incident transverse to the longitudinal axis of the blocks. In addition, secondary calibration of all blocks was performed with LED pulsers and $^{241}\text{Am-NaI}$ light sources permanently attached to each block of lead glass. This secondary calibration was performed before and after each ISR run (typically 16 to 60 hours). Any changes in counter output were determined, and the energy calibration of the blocks was corrected.

The data reported here correspond to an integrated luminosity of $1.2 \times 10^{36} \text{ cm}^{-2}$. The event trigger required at least four lead glass counters in the SP, S, F1 and F2 units to have a deposited energy of at least 300 MeV. The energy threshold for all blocks was set at 50 MeV. To reduce the possibility that a single gamma-ray or

TABLE 1
Solid angle of lead glass arrays, total solid angle and solid angle used for triggering and multiplicity determination

Unit	Total solid angle (sr)	Solid angle used (sr)
SP	0.519	0.219
S	0.559	0.233
F1	1.452	0.618
F2	1.602	0.687
U1	0.148	0.148
U2	0.144	0.144
U3	0.115	0.155

charged particle could contribute more than once to the trigger, only alternate counters were connected to the trigger system. For the SP unit 27 trigger counters were arranged in a checker board pattern; the counters at the ends of each row were excluded from the trigger. The S, F1 and F2 units each contained eight trigger counters. The solid angle subtended by each unit in the center of mass as well as the trigger solid angle is listed in table 1.

Signals from the trigger counters were input to two 32 channel logic units that gave outputs for coincidences of order 1, 2, 3 and 4. Two of these logic units were connected to form the event trigger which is represented by

$$\text{TRIG} = \sum_{n=0}^4 \text{SP}_n \cdot (\text{S} + \text{F1} + \text{F2})_{4-n},$$

where $\text{SP}_n \cdot (\text{S} + \text{F1} + \text{F2})_{4-n}$ denotes a coincidence between any n trigger blocks of the SP unit with any $4 - n$ trigger blocks in the S, F1 and F2 units.

A coincidence between the R1 and R2 beam counters was not required during data acquisition. However the time of flight information from these counters was used during data analysis to select events originating in the interaction region.

3. Data analysis

A preliminary check was made of the signals in the SP unit. If five contiguous counters in a single row had energy above the energy cut of 50 MeV, the event was rejected on the basis that it might have resulted from the lead glass array having been hit from the side. Investigation of many such events showed that such patterns usually included counters on the ends of the array and were more common for rows of lead glass near the plane defined by the two beams. Events of this type comprised less than 0.2% of our data.

The blocks of the SP and U3 units were scanned column by column. When a block having energy above 50 MeV was encountered a 3×3 sub-array having that block at the center was scanned. If the central block had the largest deposited energy, the energy in all blocks of the 3×3 array was summed to give the energy of a "cluster". To avoid using information more than once, the energy in all blocks of the 3×3 array was then set to zero. If the central block did not have the largest energy of the 3×3 array, the scan of the main array was continued. Only clusters having the largest deposited energy in the trigger blocks were included when determining the event multiplicity.

In the S, F1 and F2 units, a particle travelling from the interaction region would traverse only four radiation lengths of lead glass. Due to the transverse mounting, each block subtended a large solid angle with respect to the interaction region. For

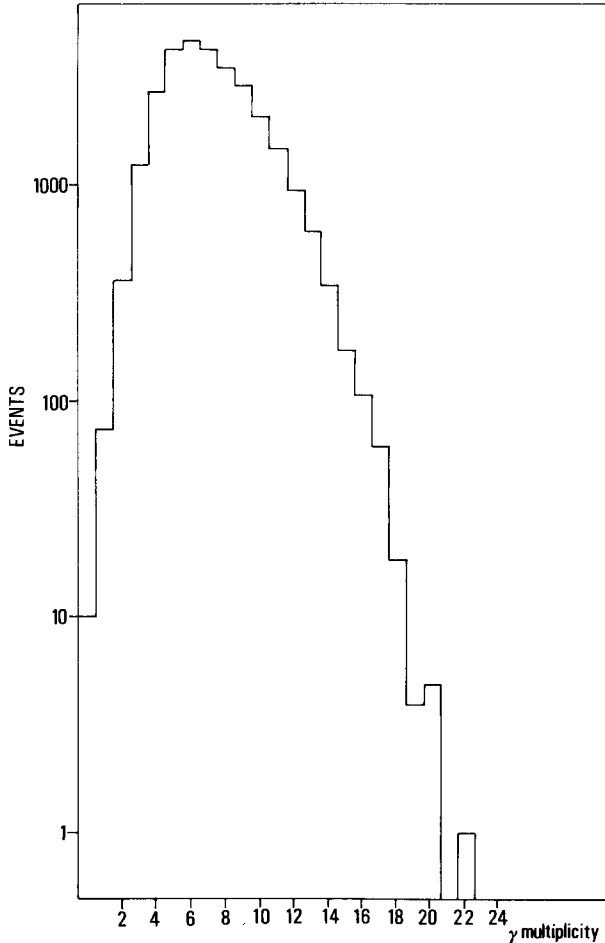


Fig. 3. Experimental multiplicity distribution.

these units the energy of an individual block was used as the “cluster” energy. As before only trigger blocks were used for determining event multiplicity.

In the U1 and U2 units the deposited energy in horizontally adjacent blocks was summed to give the “cluster” energy, while the energy deposited in blocks of different rows was interpreted as being due to separate “clusters”.

In all but the U1, U2 and U3 units a “cluster” was attributed to a charged particle if the appropriate scintillation counter fired and wires intercepted by the projection of the edges of the lead glass block to the interaction region in several wire planes showed signal.

In the U1, U2 and U3 unit a “cluster” was attributed to a charged particle if the scintillation counter in front of the lead glass block fired.

Gamma-ray multiplicity was determined by the number of neutral clusters associated with the trigger counters of the SP, S, F1 and F2 units and neutral clusters associated with all of the blocks of the U1, U2 and U3 units. The gamma-ray multiplicity distribution obtained by the above analysis is shown in fig. 3. The distribution peaks above our trigger multiplicity and then decreases rapidly with increasing multiplicity.

4. Results

It has been suggested by Ruderman and Zwanziger [3] that a possible source of events with very high photon multiplicity will be the production of a magnetic monopole-antimonopole pair. In fact if a monopole-antimonopole pair is created with insufficient relative energy to escape each other, they will drift together and annihilate.

The number of produced photons roughly estimated to be of the order of one hundred [3] depends primarily on the magnetic pole strength g which must be quantized so that

$$g = ng_0, \quad g_0 = \frac{\hbar c}{2e}, \quad n = 1, 2, 3, \dots$$

This mechanism provides a possible explanation for a few anomalous events in emulsion exposed to cosmic rays where are observed jets of pure photons [4].

A search of this kind of events has also been done with negative results at smaller value of \sqrt{s} with a neutron beam of 100–300 GeV [5].

Recent estimate of production of pole-antipole in pp interactions at ISR energies based on the renormalization group improved quark parton model, yield for a 10 GeV monopole mass a cross section of $2 \times 10^{-34} \text{ cm}^2$ [6].

To investigate the scenario by which monopole pairs or other massive pairs could decay via the emission of a large number of gamma-rays, a Monte Carlo calculation was performed to simulate how our detector would respond to gamma-rays gener-

ated by this process. Gamma-rays were generated with an isotropic distribution in the rest frame of pairs of particle having mass M with an energy spectrum described by [7]

$$N(E_\gamma) = \frac{E_\gamma^2}{e^{E_\gamma/KT} - 1},$$

where

$$\frac{1}{KT} = \frac{1}{M} \left| \frac{4.32}{\pi} \left(\frac{g^2}{\hbar c} \right)^3 \right|^{1/2},$$

derived from a black-body model for the photon shower produced in the annihilation.

In such a scheme the average number of photons $\langle n_\gamma \rangle$ turns to be 32, 59, 91, 124 for $n = 2, 3, 4, 5$, respectively. We have also generated the photons with a gaussian energy spectrum having an average energy $\langle E_\gamma \rangle = 2M/\langle n_\gamma \rangle$ and a FWHM of 0.2, 0.4, 0.8 $\langle E_\gamma \rangle$. The final results on the upper limits do not change significantly. To assure momentum conservation, gamma-rays were produced in pairs having equal energy and opposite directions in the rest frame of the pair. The momentum distribution of the pole-antipole pair in the pp system has been obtained assuming a ‘‘central’’ production mechanism with a differential cross section of the kind

$$E \frac{d^3\sigma}{d^3p} \propto (1 - |x|)^\alpha e^{-\beta p},$$

where

$$x = \frac{p_L}{p_{L \text{ MAX}}},$$

similar to that of the heavy mass hadronic states produced in pp collisions.

Here we present only the upper limits for the production cross section obtained with $\alpha = 4$ and $\beta = 2$. When α and β are moved within the intervals $0 < \alpha < 5$, $0 < \beta < 4$, the upper limits vary at most by a factor 1.5.

The gamma-rays were then transformed on the laboratory system and were followed to determine whether or not they would be intercepted by the detector. If a gamma-ray hit the detector, the deposited energy in the hit block was increased by the energy of the gamma-ray. The photon conversion in the material before the lead glass (beam pipe, chambers, etc.) has been taken into account. The total thickness of these materials was 2% of a radiation length for perpendicular crossing. After the total mass of the pair was radiated, the event was analyzed using the same procedure of the analysis.

Two tests were made: (a) To identify and reject events having five contiguous counters in any row of the SP unit with energy greater than our energy cut of 50

TABLE 2
90% confidence level upper limit for the production cross section of annihilating pole-antipole pairs versus monopole strength $g = \mu g_0$

$2M$	$n = 2$	$\langle n_\gamma \rangle = 32$	$n = 3$	$\langle n_\gamma \rangle = 59$	$n = 4$	$\langle n_\gamma \rangle = 91$	$n = 5$	$\langle n_\gamma \rangle = 124$	
(GeV)	$\langle n_\gamma \rangle_{\text{obs}}$	ϵ	σ (cm ²)	$\langle n_\gamma \rangle_{\text{obs}}$	ϵ	σ (cm ²)	$\langle n_\gamma \rangle_{\text{obs}}$	ϵ	σ (cm ²)
15	9.5	0.33	3.4×10^{-34}	13.4	0.30	2.0×10^{-34}	16.2	0.16	1.3×10^{-34}
20	10.2	0.46	2.5×10^{-34}	13.2	0.57	1.0×10^{-34}	16.3	0.52	3.7×10^{-35}
30	10.1	0.59	2.0×10^{-34}	13.1	0.82	7.0×10^{-35}	16.3	0.88	2.2×10^{-35}
40	10.0	0.62	1.9×10^{-34}	13.0	0.88	6.8×10^{-35}	16.4	0.96	2.1×10^{-35}

$\langle n_\gamma \rangle$ = average number of γ -rays emitted according to the adopted model [7].

$\langle n_\gamma \rangle_{\text{obs}}$ = average number of γ -rays expected to be detected.

ϵ = trigger efficiency.

M = monopole mass.

MeV. (Very few events of this type were generated by the Monte Carlo program.) (b) To determine whether the trigger condition of having at least 300 MeV of energy in any four of the selected trigger blocks was satisfied. (For low M values and high n , more than one gamma-ray is necessary to deposit the energy required to fire our trigger discriminators.) We assumed that any gamma-ray hitting the front surface of a block was totally absorbed in that block.

Then the same criteria used in the data analysis were adopted to determine the photon multiplicity. The values of ϵ , trigger efficiency and $\langle n_\gamma \rangle_{\text{obs}}$, average photon multiplicity as determined by the Monte Carlo are given in table 2.

As an example the results of the Monte Carlo simulation, on the photon multiplicity distribution for $M = 15$ GeV, are shown in fig. 4.

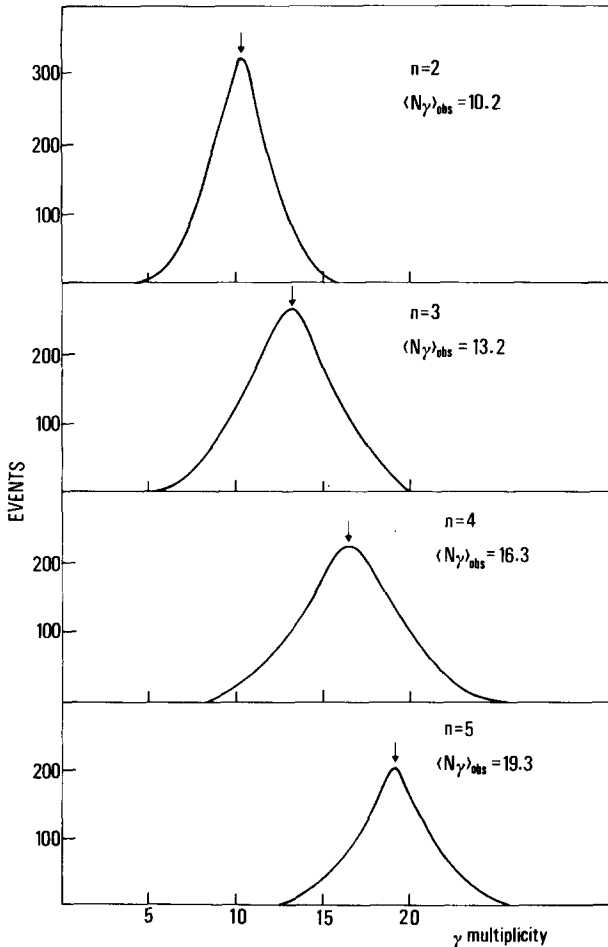


Fig. 4. Expected photon distribution for various values of monopole strength n for $2M = 30$ GeV.

From our integrated luminosity of $L = 1.2 \times 10^{36} \text{ cm}^{-2}$ and the probability ϵ computed with the Monte Carlo, that gamma-rays from the decay of pairs of particles could trigger our detector, we obtain 90% confidence level upper limits to the production cross section for monopole or heavy mass pairs as a function of the pair mass.

In this derivation we make the dynamical assumption that the requirement of coincidence between R1 and R2 used to define the interaction region does not change the relative efficiency of the pole-antipole events with respect to the normal hadronic interactions. In these interactions this efficiency is ~ 0.7 and has been included in the computation of the upper limits for the cross section.

Although this assumption can not be justified by a specific dynamical model, it should be remarked that it is consistent with the central production model used above.

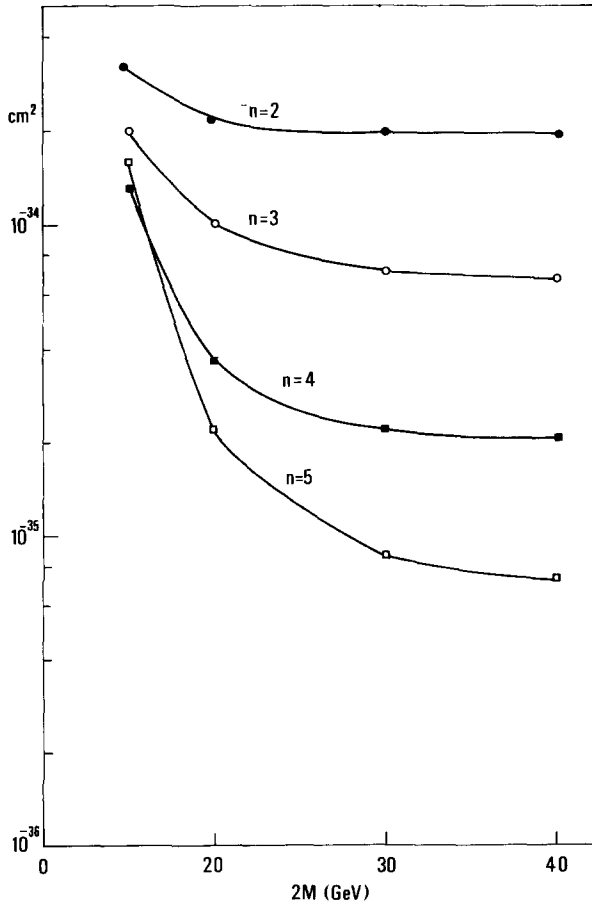


Fig. 5. Upper limits for monopole production versus monopole mass for monopole strength $n = 2, 3, 4, 5$.

The upper limits for the production cross sections are listed in table 2 and shown in fig. 5. These upper limits were obtained assuming that the background can be represented by a smooth curve. In case of $n = 5$ the upper limit was computed assuming that all events above γ -multiplicity 21 were due to the signal. Moreover we make the hypothesis that the pole-antipole pair is produced without any associated π^0 . This is a pessimistic assumption because other detected γ -rays will shift the distributions of fig. 4 toward higher average multiplicities where the background is smaller.

In conclusion we have seen no evidence for high multiplicity gamma-rays events due to decay of a high mass states.

We express our thanks to the staff of the ISR Division and to Mr. G. Basti, A. Donnini and S. Guerra for their technical help. We would like to record our sincere appreciation for the work of Dr. Bruno Baldo who contributed much to the success of this experiment. He died prematurely on June 26, 1981.

References

- [1] E. Amaldi, M. Beneventano, B. Borgia, A. Capone, F. de Notaristefani, U. Dore, F. Ferroni, E. Longo, L. Luminari, P. Pistilli, I. Sestili, G.F. Dell, H. Uto, L.C.L. Yuan and J. Dooher, *Nuovo Cim. Lett.* 19 (1977) 152; 20 (1977) 409
- [2] E. Amaldi, M. Beneventano, B. Borgia, A. Capone, F. de Notaristefani, U. Dore, F. Ferroni, E. Longo, L. Luminari, P. Pistilli, I. Sestili, G.F. Dell, H. Uto, L.C.L. Yuan, G. Kantardjian and J. Dooher, *Nucl. Phys.* B150 (1979) 326
- [3] M.A. Ruderman and O. Zwanzinger, *Phys. Rev. Lett.* 22 (1969) 146
- [4] M. Schein, D.M. Haskin and M.C. Glasser, *Phys. Rev.* 95 (1954) 855;
A. Debenedetti, C.M. Garelli, L. Tallone and M. Vigone, *Nuovo Cim.* 2 (1955) 220;
M. Koshiba and F. Kaplon, *Phys. Rev.* 100 (1955) 327;
L. Barbanti Silva, C. Bonacini, C. Depietri, L. Fori, G. Lovera, R. Perilli Fedeli and A. Roveri, *Nuovo Cim.* 3 (1956) 1465;
G.B. Collins, J.R. Ficencic, D.M. Stevens and W.P. Trower, *Phys. Rev.* D8 (1973) 982
- [5] D.L. Burke et al., *Phys. Lett.* 60B (1975) 113
- [6] L.E. Roberts and J.P. Dooher, *Adelphy multigamma report no.* 12 (June, 81)
- [7] J.L. Newmeyer and J.S. Trefil, *Nuovo Cim.* 8A (1972) 703